ANL/CP--70627

DE91 010629

TRITIUM RETENTION AND RELEASE ANALYSIS FOR U.S.-ITER BLANKET*

M.C. Billone and C.C. Lin
Argonne National Laboratory
Argonne, IL 60439 USA

H. Attaya and Y. Gohar
Fusion Power Program
Argonne National Laboratory
Argonne, IL 60439 USA

November 1990

* Work supported by the Office of Fusion Energy, U.S. Department of Energy under Contract Number W-31-109-Eng-38.

TRITIUM RETENTION AND RELEASE ANALYSIS FOR THE U.S.-ITER DRIVER BLANKET*

M.C. Billone and C.C. Lin
Argonne National Laboratory
9700 S. Cass Ave., Bldg. 212
Argonne, IL 60439 USA
(708) 972-7146

H. Attaya and Y. Gohar
Argonne National Laboratory
9700 S. Cass Ave., Bldg. 205
Argonne, IL 60439 USA
(708) 972-4484

ABSTRACT

The U.S. design for the ITER tritium-breeding blanket consists of layers of Be multiplier, stainless steel cladding, and Li_2O ceramic breeder. Tritium is recovered from the ceramic breeder by purging it with He + 0.2% H_2. Models have been developed to describe the purge-flow thermal-hydraulics and gas reactions and the tritium retention/release due to lattice diffusion, desorption/adsorption, solubility/precipitation, and percolation through interconnected porosity. These have been incorporated into the steady-state code TIARA for the purpose of performing design calculations for Tritium Inventory and Release Analysis. Transient calculations for pulsed operation are done with a modified version of the DISPL code. The results of both steady-state and transient analyses for tritium retention and release are given for anticipated ITER operating conditions.

I. INTRODUCTION

The U.S.-ITER driver blanket consists of Li_2O solid breeder zones, Be multiplier/thermal-resistance zones, annealed 316 stainless steel structural and cladding material, and low pressure water coolant.[1] The solid breeder layers (2 outboard and 1 inboard) are separated on each radial side from the water coolant by steel cladding layers and Be layers.

Figure 1 shows a schematic of a solid breeder plate with stainless steel cladding and semi-circular grooves at the breeder/cladding interface for toroidal flow of the He (+0.2% H_2) purge stream. The radial thickness of the breeder plates is 8 mm for the two outboard breeder zones and 10 mm for the inboard zone. The toroidal span of the plate is ~1 m. Based on detailed modeling and experimental results, the Li_2O is specified to be 80% dense material with 20-μm grain diameter, 0.05 m^2/g specific surface area, and 95% ^6Li enrichment. The breeder layer is segmented into cubic blocks to minimize thermal-stress cracking. Table 1 summarizes the main fabrication and operational parameters for the ITER design.

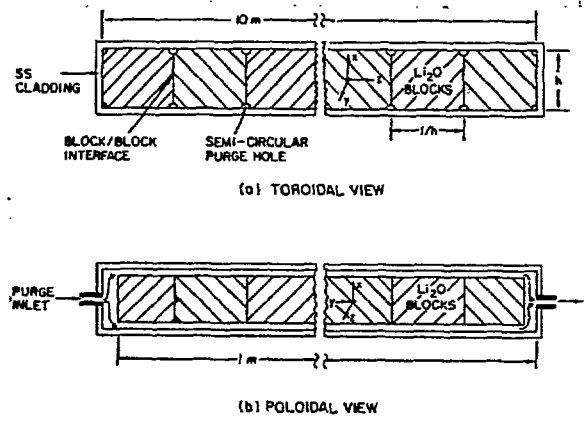

Figure 1. Schematic of Li_2O breeder plates for sintered-product design.

In this paper, the models and analytical methods used to calculate purge flow hydraulics/chemistry and tritium inventory are described for both steady-state and pulsed operation. The Tritium Inventory and Release Analysis code TIARA is used to perform whole blanket calculations for steady-state temperatures and generation rates. The DISPL2 code[2] is used to perform local transient calculations to study the effects of pulsed temperature and generation rate on tritium release.

* Work supported by the Office of Fusion Energy, U.S. Department of Energy under Contract Number W-31-109-Eng-38.

Table 1. Summary of Solid-Breeder Parameters for ITER. Breeder is Li_2O: 95% enriched, 80% dense, 20 μm grains, sintered blocks.

Parameter	Inboard	Outboard	Total
# of zones	1	2	---
Thickness,mm	10	8	---
Mass, MT	2.07	10.53	12.6
Tritium gen. rate, g/day			
Physics	21.5	105.6	127
Technology	18.5	92.7	111
Temperatures (min/max) at full power °C			
Physics	493/603	499/609	493/609
Technology	442/527	448/536	442/536
He purge			
Flow rate, mol/s	0.53	2.71	3.24
Avg. temp, °C	450	450	450
Inlet press., MPa	0.2	0.2	0.2
Outlet press., MPa	0.1	0.1	0.1
H_2, vol.%	0.2	0.2	0.2
H/T	29.8	30.5	30.4

II. MODELS AND PROPERTIES

A. Purge Flow Hydraulics and Chemistry

Two important aspects of the purge flow analysis are the He flow rate (relative to the tritium generation rate) and the outlet protium-to-tritium ratio (H/T). The He flow rate is chosen to limit the maximum local moisture (H_2O + HTO + T_2O) level to less than the value which would cause precipitation of separate phase lithium hydroxide (LiOH/ LiOT).[3-4] At low temperatures, this precipitation acts as a chemical "trap" for tritium retention. For temperatures above the melting point (471°C), the presence of separate-phase lithium hydroxide can cause undesirable sintering and grain growth in Li_2O, as well as mass transport at even higher temperatures. Figure 2 shows the solubility limit of hydroxide in Li_2O.[3-4] In the current design analysis, the maximum local moisture pressure is limited to ~10 Pa, corresponding to a critical temperature of ~360°C. The minimum local He (flow rate)-to-tritium (release rate) is determined to be $He/T_2 \sim 10^4$ to limit the maximum moisture pressure to ≤10 Pa.

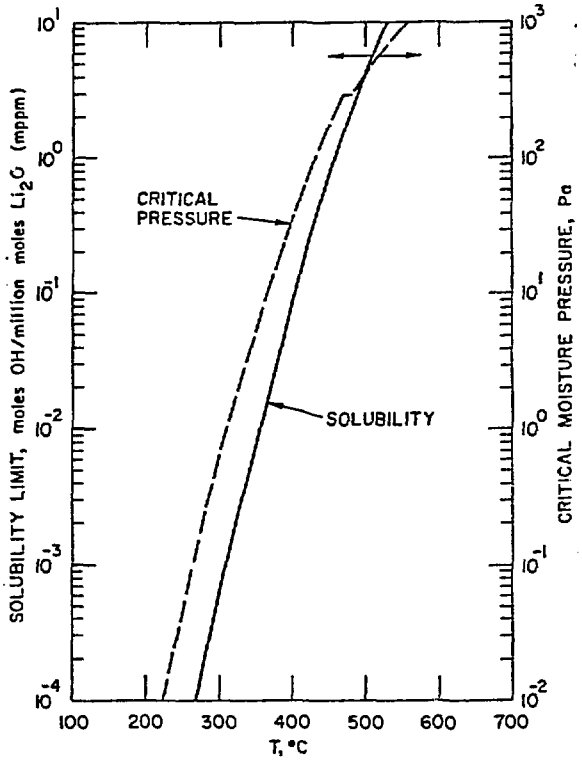

Figure 2. Hydroxide solubility limit and critical moisture pressure in Li_2O.

With the desired He flow rate established, the size and number of the purge flow grooves are selected based on the desired purge inlet/outlet pressure. Using elementary permeation theory in the viscous flow regime and the properties of He gives the following relationship[3] between purge hole diameter (d_p in m), number of complete purge holes/m^2 (n_p), outlet pressure (P_o in MPa), pressure drop (ΔP in MPa) along the 1-m flow path and gas temperature (T in K) as:

$$d_p = 1.185\times10^{-4}\, T^{0.41}\, [n_p\, \Delta P\, (P_o+\Delta P/2)]^{-0.25} \quad (1)$$

For sample design calculations, assume $n_p=10^4$ complete holes/m^2 (1 hole/cm^2) and T=723 K. Then for P_o = 0.1 and ΔP = 0.13, d_p = 4.6 x 10^{-4} m (0.46 mm). If a lower outlet pressure and pressure drop are required, then the purge hole diameter must be increased. For example, for P_o = 0.05 MPa and ΔP = 0.0017 MPa, then d_p = 1 x 10^{-3} m (1 mm). Thus, 0.46 ≤ d_p ≤ 1 mm should cover all of the design ranges of interest.

The next step in the purge flow analysis is to establish models to determine the optimum H/T ratio based on gas chemistry. Excellent tritium release has been achieved experimentally with protium levels of 0.1-1% in 1-atm He purge. A mathematical model[3] has been developed based on thermodynamic equilibrium to determine mole fractions of H_2, HT, H_2O, HTO, and T_2O in the purge as a function of molar tritium release rate, inlet H_2 flow rate, inlet H_2O flow rate, temperature and position. Figure 3 shows the exit molar flow rates at 400°C. All results are normalized to the molar generation rate of T_2, which at steady-state is assumed to be equal to the release rate to the purge. The minimum H_2/T_2 ratio for design is chosen to have a value of 20. This corresponds to a protium level of ~0.2 vol. % in the inlet He purge.

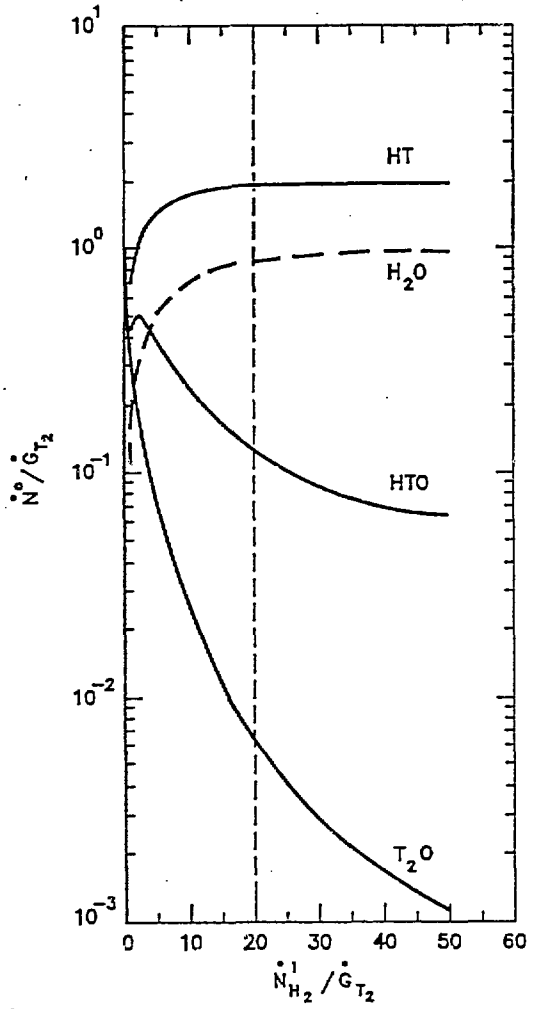

Figure 3. Effect of protium purging on chemistry of purge gases. Calculation performed for 400°C.

B. Tritium Models and Properties

Models and properties are needed for tritium diffusion (lattice and grain boundary), adsorption/desorption, and solubility/precipitation, as well as gas-phase percolation through the interconnected porosity. The lattice diffusion coefficient (D in m^2/s) for tritium in lightly-irradiated Li_2O is well established.[4]

$$D = 6.81\times10^{-7} \exp(-84.8\ kJ\cdot mol^{-1}/RT) \quad (2a)$$

for $T \geq 623K$ (350°C) and

$$D = 1.41\times10^{-3} \exp(-124.5\ kJ\cdot mol^{-1}/RT) \quad (2b)$$

for $T < 623$ K,

where

$R = 8.314\times10^{-3}$ kJ/mol-K.

The transition temperature, as well as the activation energy for the low temperature branch (Eq. 2b), increases as a function of fluence.[5] However, for Li_2O with 20-μm grain diameter in the ITER operating range (Table 1), the bulk diffusion contribution to the total inventory is <<1 g for the 12.6 MT of Li_2O.

Tritium diffusing through the grains of 80% Li_2O arrives both directly and indirectly (by means of grain boundary diffusion) at the pore/solid interfaces associated with the interconnected porosity. No data are available for determining the grain boundary diffusion coefficient. For the purpose of this work, grain boundary diffusion is assumed to be a fast transport mechanism relative to the decomposition/desorption which occurs at the pore/solid interface. Tritium desorbs from the solid as a tritiated molecule. The model adopted for this effect is based on Kudo's[6] observations for the thermal decomposition of LiOH, LiOD, and LiOT. He found that the moisture release from lithium hydroxide obeys first order kinetics in the temperature range of 257-417°C. This leads to the following steady-state model for fractional surface coverage (θ) of OH and OT:

$$\theta_{OH} + \theta_{OT} = (\dot{g} \times 10^{-6}/3)/(a_{fs}\ n_{max}\ k_d) \leq 1 \quad (3)$$

where

$\dot{g}$ is the tritium generation rate in wppm/ s, a_{fs} is the specific surface area in m^2/g, n_{max} is the maximum hydroxide surface coverage (1.66×10^{-5} moles/m^2), and k_d (in 1/s) is given by

$$k_d = \exp\left[(19.0\pm1.5) - (122\pm8)\ kJ\cdot mol^{-1}/RT\right] \quad (3a)$$

The OH surface coverage is determined as a function of temperature and H_2O and H_2 partial pressures (for H/T >>1) from solubility data by assuming that the "concentration" in the surface reaction layer (2.73×10^{-10} m) equals the concentration in the bulk.

The solubility of hydrogen (i.e., OH) in Li_2O is well established for the Li_2O/H_2O system in the temperature range of 713-1273 K. However, for Li_2O/H_2, there is a high degree of uncertainty (> factor of 4).[8] Figure 4 summarizes the results from several authors.[8-10] Also shown in Fig. 4 are the extrapolated results from Tetenbaum et al.[11] and Norman and Hightower[12] for the Li_2O/H_2O system. The solubility limit is based on the work of Tetenbaum and Johnson.[13] The O'Hira et al. results (476 ≤ T ≤ 963 K) are used in this present work because tritium retention was measured directly in their samples. The resulting equation for solubility (S_{OH} in atom parts H per million Li_2O molecules, appm) due to both H_2 and H_2O partial pressures (Pa) is

$$S_{OH} = 10^{-A}\left(9.864 \times 10^{-6}\ P_{H_2O}\right)^B + 173\exp(-2950/T)\ P_{H_2}^{1/2} \quad (4)$$

where

$A = 11.667 - 2.502 \times 10^{-2}\ T + 9.62 \times 10^{-6}\ T^2$

$B = 0.427 + 1.7 \times 10^{-4}\ T.$

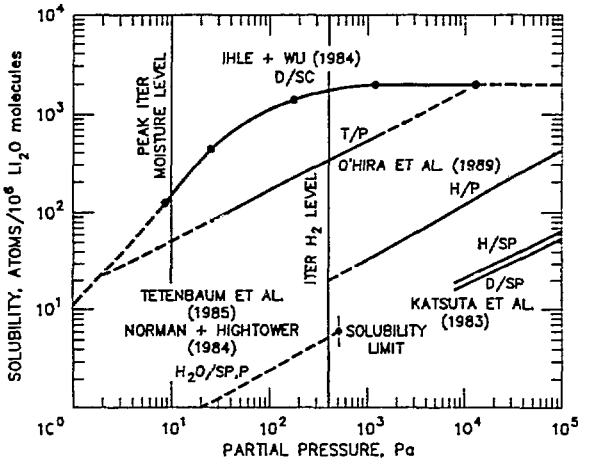

Figure 4. Summary of experimental results for protium (H), deuterium (D), and tritium (T) solubility in single crystal (SC), sintered product (SP) and powdered (P) Li_2O at 515°C.

In the steady-state calculations, adsorption is not distinguished from solubility. It is assumed that the concentration in the bulk (due to gas partial pressures) is equal to the concentration in the surface layer. This assumption will be re-examined in future work.

Equation 4 can be rewritten to find the tritium (OT) solubility in Li_2O as a function of T_2O and HT partial pressures. The T_2O and HT partial pressures in the purge stream at each toroidal location are calculated in the analysis for the purge chemistry. The increase in these quantities through the radial thickness of the breeder is calculated using a standard percolation model.[3]

III. COMPUTER CODES

A. Steady State Analysis

TIARA is a special purpose computer code developed to determine purge gas chemistry and tritium inventory under steady-state operating conditions. Input to the TIARA code includes geometry (radial thickness and toroidal length), microstructural parameters (porosity, grain size, and specific surface area), purge inlet conditions (temperature, partial pressures, and flow rates), tritium generation rate (in wppm/s), and a one-dimensional (radial thickness) temperature profile. It basically solves for the two-dimensional (radial-thickness, toroidal) gas partial-pressure profiles, the purge outlet partial pressures and flow rates, and the tritium inventory in the solid due to bulk diffusion, desorption, solubility/adsorption and precipitation, as well as the tritium inventory in the gas phase. The calculation is performed for a poloidal cross-section (Fig.1). It is repeated at several poloidal locations. The results are combined (externally to the code) to give whole-blanket inventories and flow rates. Currently, only the Li_2O models and properties in Section II are incorporated into TIARA.

B. Transient Analysis

During pulsed operation the tritium and heat generation rates will have a time-dependence. For ITER operation during the physics phase, short (600-s) pulses are planned: 20-s up-ramp to power, 400-s flat burn, 20-s down-ramp, and 160-s dwell time at zero power. A longer burn time of 2290-s is envisioned for the technology phase. During the rise to power, the breeder temperatures will lag the power rise, and the tritium release rate will lag the temperature increase.

The DISPL2 code is used for the transient tritium transport calculations. This code is an advanced version of the DISPL1 code.[2] It is a general-purpose transient code for one and two spatially dimensioned kinetics-diffusion problems. Rectangular, cylindrical and spherical coordinate system options are available. Cyclic generation-rate and temperature histories were built into the user subroutines, which also contain the material properties (e.g., diffusion and desorption coefficients).

The equivalent spherical-grain model is used to represent a local point within the breeder. Repeated calculations are performed across the plate thickness to obtain the results for a thickness slice at a particular toroidal/poloidal location. Based on the steady-state results, desorption is the rate-limiting mechanism for tritium release and the major inventory component at low temperature while solubility is the major inventory component at higher temperatures. Diffusion is relatively fast and has an insignificant effect on the inventory. Therefore, in order to make the long-time transient calculation consistent with the steady-state calculation, the desorption component is modeled rigorously and parameters in the diffusion model are modified to give the correct long-time solubility component. This approach was verified by running DISPL2 for a long flat-burn time and comparing this solution to the TIARA solution.

IV. RESULTS AND DISCUSSION

A. Steady State Results

TIARA was run for three inboard and three outboard poloidal locations. These locations corresponded to the midplane (peak power), the top or bottom of the blanket (minimum power), and an intermediate position corresponding to the average power and tritium generation rates. The calculated purge outlet partial pressures and flow rates for the technology phase operating conditions are shown in Table 2. Notice that the maximum local moisture pressure occurs at the purge outlet of the midplane outboard breeder plate #1 (closest to the plasma). Its value (10.7 Pa) is reasonably close to the design goal of 10 Pa. It corresponds to a critical temperature for initiating LiOH(T) precipitation of 368°C. Thus, the thermal margin for this design is 80°C. Also, the corresponding H/T ratio at this location is 21, while the average value for the whole blanket is ~30.

The local tritium concentrations (in wppm) and the overall inventories (in g) calculated by TIARA for each mechanism are given in Table 3 for technology phase operating conditions. The overall inventory is only ~14 g with upper and lower bound values of 45 and 6 g, respectively. Desorption is predicted to be the rate-limiting release mechanism and to contribute most to the inventory during technology phase operation (442-536°C). Similar calculations for the higher temperature physics phase yielded 2.6 g, with upper and lower bound values of 9.5 and 2.5 g, respectively. At physics phase temperatures (493-609°C), solubility is the major tritium-inventory component.

B. Transient Results

Two cases were run with the DISPL2 code to study the effects of generation-rate and temperature cycling on the tritium inventory. In the first case, the anticipated pulsing for the technology phase was simulated. In general, this is difficult to do with the simplistic method adopted, because of the toroidal and radial coupling through the gas phase. However, as desorption is rate limiting and the parameters which are used in the model are relatively constant in the toroidal (e.g., temperature and H_2 partial pressure) and radial thickness (e.g., H_2 partial pressure) directions, reasonable results were obtained by performing separate local analyses at points along the thickness direction. The technology phase results are shown in Figure 5 for the first breeder plate at the outboard midplane position. Each cycle is a total of 2490 s. The results are normalized to the TIARA steady-state inventory (I_{ss}) at this location and correspond to the times at the end of the flat burn for each cycle. With the long technology-phase pulses, the cycling causes only a 17% increase in inventory over the steady-state results. This case corresponds to a breeder (T_{min}, T_{max}) = (138°C, 140°C) at the beginning of the ramp to power, end-of-flat-burn temperatures (T_{min}, T_{max})=(453°C, 536°C), and a generation rate of 12.8 wppm/day.

The transient results for the shorter (600 s) physics-phase pulses are shown in Figure 6. For this case, the reference steady-state inventory is smaller than for the technology phase and the increase due to the transient effects of cycling is only ~25%. Thus, the transient effects due to the pulsed nature of operation for both the physics and technology phases are small relative to the uncertainties in the model parameters. This case corresponds to a breeder (T_{min}, T_{max}) = (142°C, 150°C) at the beginning of the ramp to

Table 2.
Summary of Purge Flow Exit Analysis for the ITER Technology Phase, with a He (+ 0.2% H_2) Flow Rate of 2.80×10^5 moles/day, an Inlet Pressure of 0.23 MPa, and an Exit Pressure of 0.1 MPa.

Parameter	Location[a]	H_2	HT	H_2O	HTO	T_2O
Partial	IB/Mid	190	13.3	6.29	0.720	0.0204
Pressure, Pa	IB/Ave	190	12.9	6.11	0.678	0.0189
	IB/Top	196	5.96	2.91	0.146	0.0018
	OB1/Mid	185	18.0	9.33	1.33	0.0527
	OB1/Ave	186	17.0	7.91	1.17	0.0439
	OB1/Top	191	12.7	5.52	0.548	0.0136
	OB2/Mid	190	13.0	6.15	0.686	0.0192
	OB2/Ave	194	8.44	4.07	0.288	0.0051
	OB2/Top	199	3.57	1.76	0.0514	0.0004
Total Flow	IB	86.1	5.86	2.77	0.308	0.009
Rate, moles/day	OB	439	28.8	13.6	1.63	0.054
	Total	525	34.7	16.4	1.94	0.063

a- Inboard (IB), outboard plate #1 (OB1) closest to the plasma, and outboard plate #2 (OB2) farthest from the plasma.

Table 3.
Local and Global Results for Tritium Inventory in Li_2O Under Steady-State Technology Phase Operating Conditions

Location[a]	Desorp.	Sol.	Diff.	Gas Phase	Total
IB/Mid (wppm)	0.658	0.129	5.96E-4	6.76E-4	0.788
IB/Ave (wppm)	0.815	0.120	6.45E-4	6.60E-4	0.936
IB/Top (wppm)	0.202	0.045	4.93E-4	3.03E-4	0.248
OB1/Mid (wppm)	1.281	0.183	7.57E-4	9.33E-4	1.466
OB1/Ave (wppm)	1.551	0.161	8.34E-4	8.82E-4	1.714
OB1/Top (wppm)	1.114	0.097	7.52E-4	5.96E-4	1.212
OB2/Mid (wppm)	0.962	0.115	7.24E-4	8.50E-4	1.079
OB2/Ave (wppm)	0.192	0.072	5.05E-4	4.27E-4	0.265
OB2/Top (wppm)	0.000	0.026	3.20E-4	1.80E-4	0.027
Total/IB (g)	1.69	0.25	0.00	0.00	1.94
Total/OB (g)	10.4	1.20	0.01	0.01	11.6
Total/IB+OB (g)	12.1	1.45	0.01	0.01	13.6

a- Inboard (IB), outboard plate #1 (OB1) closest to plasma, and outboard plate #2 (OB2) farthest from plasma.

power, end-of-flat-burn temperatures (T_{min}, T_{max}) = (487°C, 584°C), and a generation rate of 15.1 wppm/day.

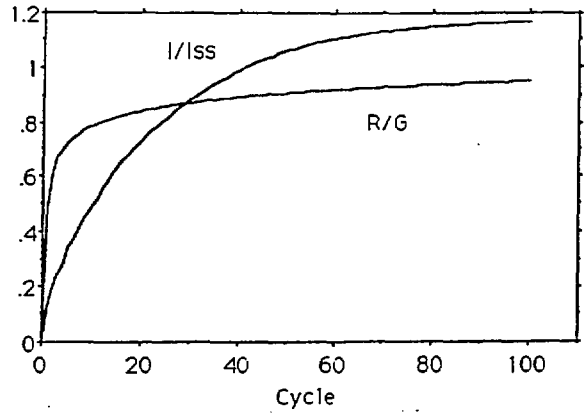

Figure 5. Tritium Inventory (I/Iss) and Release (R/G) for Technology Phase (Outboard Midplane). Iss = 1.464 wppm.

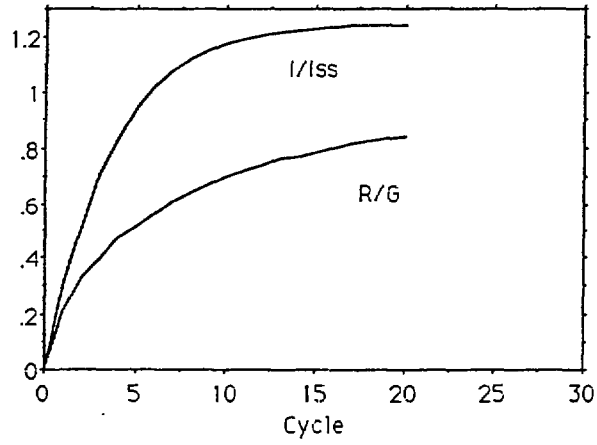

Figure 6. Tritium Inventory (I/Iss) and Release (R/G) for Physics Phase (Outboard Midplane). Iss = 0.225 wppm.

C. Discussion

Based on a summary of the data for hydrogen isotope behavior in Li_2O, the largest uncertainty (factor of 4) appears to be associated with hydrogen solubility for the Li_2O/H_2 system. The model with the largest uncertainty is the surface desorption model. Not only does this model depend on the amount of protium adsorbed to the surface (which is highly uncertain), but the model itself needs further development and improvement. In general when the steady state models are compared to the mean residency times and implied inventories from in-reactor purge flow tests at T > 300°C, the model tends to predict inventories higher than those measured directly or implied by the data. As most of the data pertain to transient release, rather than steady-state inventory, future efforts will be focused on model validation using the transient DISPL2 code.

Two cycling cases were run with the transient option of the DISPL2 code. An equivalent sphere representation was used to model bulk and surface phenomena. While it was somewhat fortunate that reasonable results were obtained for these specific cases without coupling the transient gas behavior to the transient bulk behavior, the DISPL2 model needs to be generalized in the near future to at lease apply to a radial slice across the thickness of the breeder. This can be done if the code is run in a 2-D mode rather than in the 1-D spherical mode. Also, solubility and the kinetics of dissolution should be incorporated formally into the code, rather than be treated in the approximate manner done here.

With regard to the transient results presented, the technology-phase temperature history starts with a breeder T_{min} of 138°C at the beginning of the ramp to power and reaches the 453°C steady-state value within the first 25% of the flat burn time. During the early low-temperature part of the cycle, particularly from 138°C to 368°C, tritium may be trapped in the solid as separate-phase LiOT. While this precipitation was not formally included in the transient model, the kinetics of the surface desorption model were so slow at these temperatures that essentially no newly generated tritium was calculated to be released during this early part of the burn cycle.

V. CONCLUSIONS

Based on TIARA calculations, the tritium inventory in the Li_2O breeder is only 14 g (6-45 g) under steady-state ITER operating conditions. The corresponding average concentration is 1.1 wppm (0.5-3.5 wppm). The major uncertainty in the calculation is in the tritium inventory due to solubility of gas-phase HT and the amount of OH surface coverage due to adsorption of gas-phase H_2. The pulsed nature of ITER operation causes both thermal and tritium transport response delays relative to the generation rate. According to DISPL2 calculations, this results in an increase of only 17% in inventory at the outboard midplane section during the technology phase. Similar calculations for the shorter-cycle, physics-phase pulses resulted in a 25% increase in

inventory relative to the steady-state value of 2.6 g. These increases are small relative to the uncertainties in model parameters.

REFERENCES

1. Y. GOHAR, M. BILLONE, H. ATTAYA, and M. SAWAN, "Neutronics and Thermal Design Analyses of the U.S. Solid Breeder Blanket for ITER," Proceedings of the 9th Topical Meeting on the Technology of Fusion Energy, Oak Brook, IL, October 7-11, 1990.

2. G.K. LEAF and M. MINKOFF, "DISPL1: A Software Package for One and Two Spatially Dimensioned Kinetics-Diffusion Problems," Argonne National Laboratory Report ANL-84-56 (September 1984).

3. M.C. BILLONE, "Purge Flow Design Analysis and Tritium Inventory Calculations for ITER Li_2O Solid Breeder Blankets," Argonne National Laboratory Report ANL/FPP/TM-245, to be published.

4. M.C. BILLONE and W.T. GRAYHACK, "Mathematical Models for Predicting Tritium Transport in Lithium Ceramics," Advances in Ceramics, Vol. 25, Fabrication and Properties of Lithium Ceramics, Amer. Ceram. Soc. (1989).

5. T. TANIFUJI, unpublished work.

6. H. KUDO, "The Rates of Thermal Decomposition of LiOH(s), LiOD(s), and LiOT(s)," J. Nucl Mater. 87 (1979) 185.

7. M. TETENBAUM, A.K. FISCHER, and C.E. JOHNSON, "An Investigation of the Solubility of LiOH in Solid Li_2O," Fusion Techn. 7 (1985) 53.

8. H.R. IHLE and C.H. WU, "The Solubility of Deuterium in Solid Li_2O," J. Nucl. Mater. 122 & 123 (1984) 901.

9. H. KATSUTA, S. KONISHI, and H. YOSHIDA, "Solubility of Hydrogen in Li_2O," J. Nucl. Mater. 116 (1983) 244.

10. S. O'HIRA, T. HAYASHI, K. OKUNO, and H. KUDO, "Tritium Dissolution in and Release from Li_2O," Fusion Eng. and Design 8 (1989) 355.

11. M. Tetenbaum, A.K. Fischer, and C.E. Johnson, "An Investigation of the Solubility of LiOH in Solid Li_2O," Fusion Techn., 7 (1985) 53.

12. J.H. Norman and G.R. Hightower, "Measurements of the Activity Coefficient of LiOH Dissolved in Li_2O(s) for Evaluation of Li_2O as a Tritium Breeding Material," J. Nucl. Mater., 122 & 123 (1984) 913.

13. M. Tetenbaum and C.E. Johnson, "Partial Pressures of H_2O Above the Diphasic Li_2O(s)-LiOH(s,l) System," J. Nucl. Mater., 126 (1984) 25.